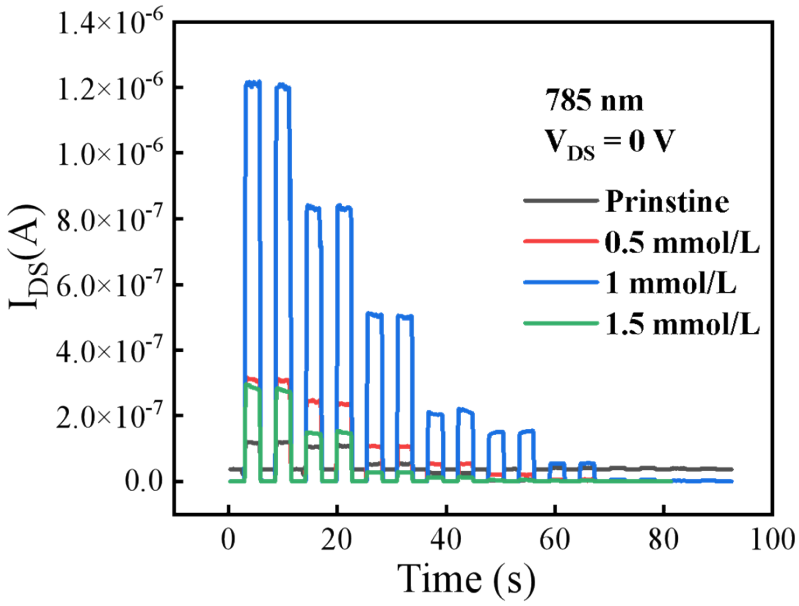

Figure S1 *The temporal photovoltaic response of the $MoTe_2/ReS_2$ photodetector under different F4-TCNQ doping concentration.*

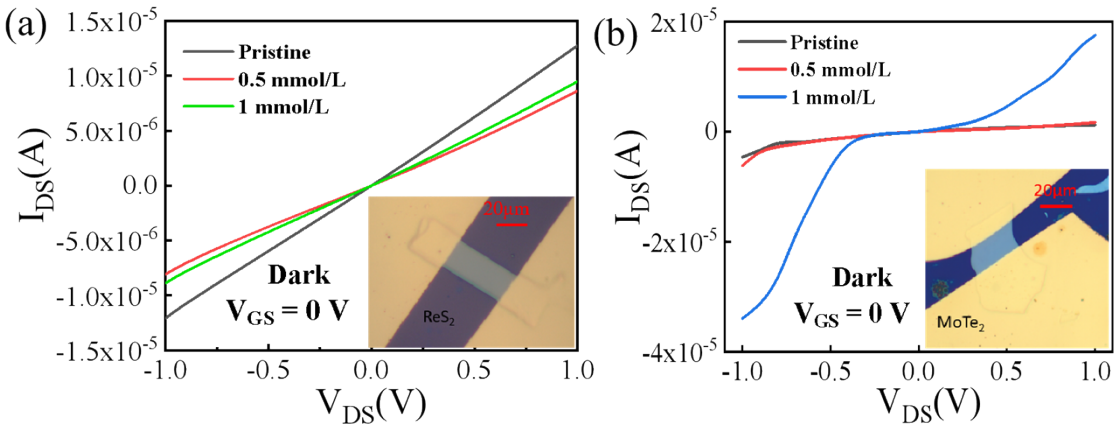

Figure S2 *(a,b) Output curves (V_{GS}=0 V) of ReS_2 FET and $MoTe_2$ FET with sandwich-like structure in dark before and after doping.*

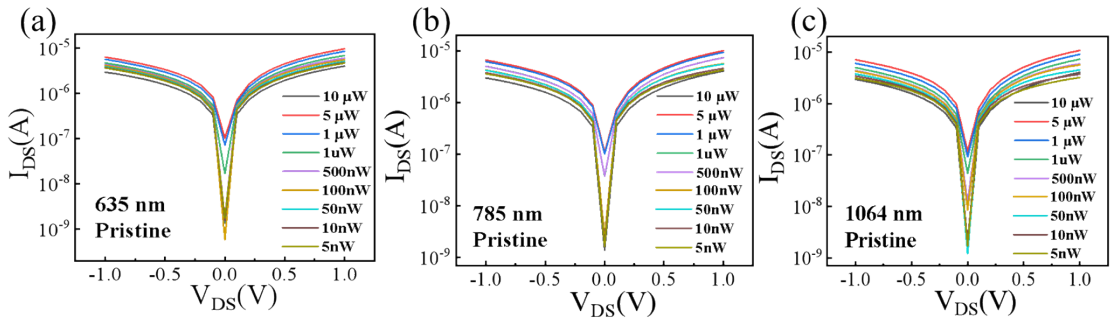

Figure S3 *(a-c) Output curves of the undoped $MoTe_2/ReS_2$ photodetector under 635, 785 and 1064 nm laser irradiation with varying optical power level.*

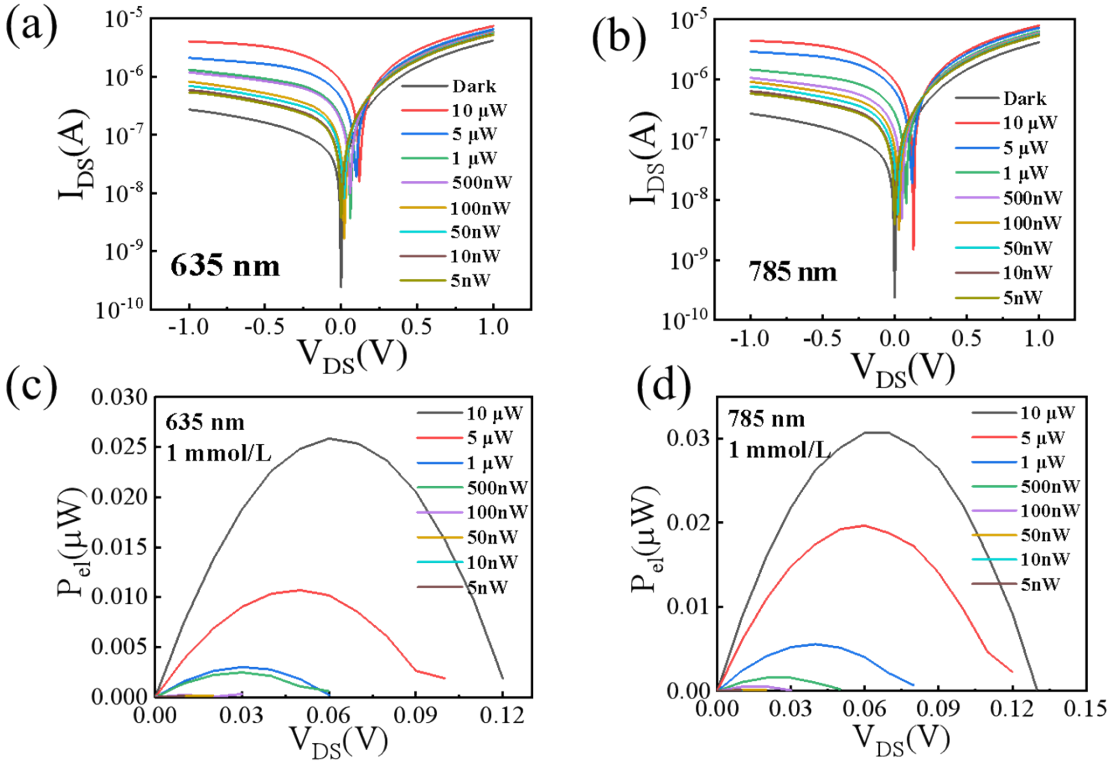

Figure S4 *(a,b) Output curves of the doped photodetector under 635, 785 nm laser irradiation with varying optical power level. (c,d) Electrical power P_{el} versus bias voltage characteristics extracted from the doped photodetector under 635, 785 nm illumination with different optical power densities.*

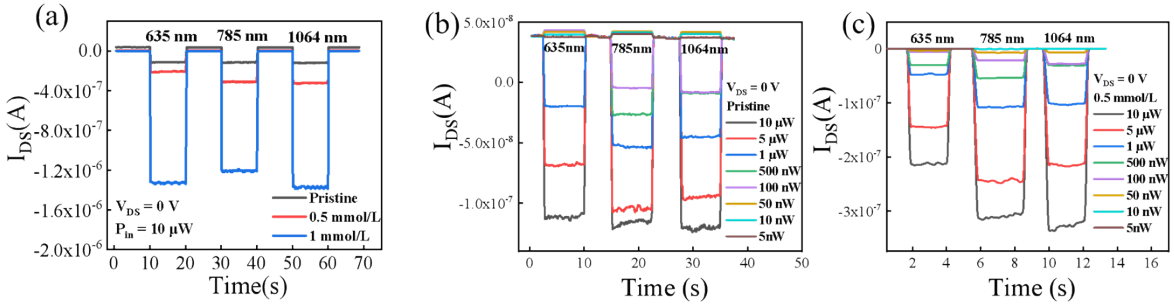

Figure S5 *(a) Temporal photovoltaic response of the WSe_2/ReS_2 photodetector before and after doping. (b,c) Temporal photovoltaic response of the photodetector undoped and doped with 0.5 mmol/L F_4-TCNQ.*

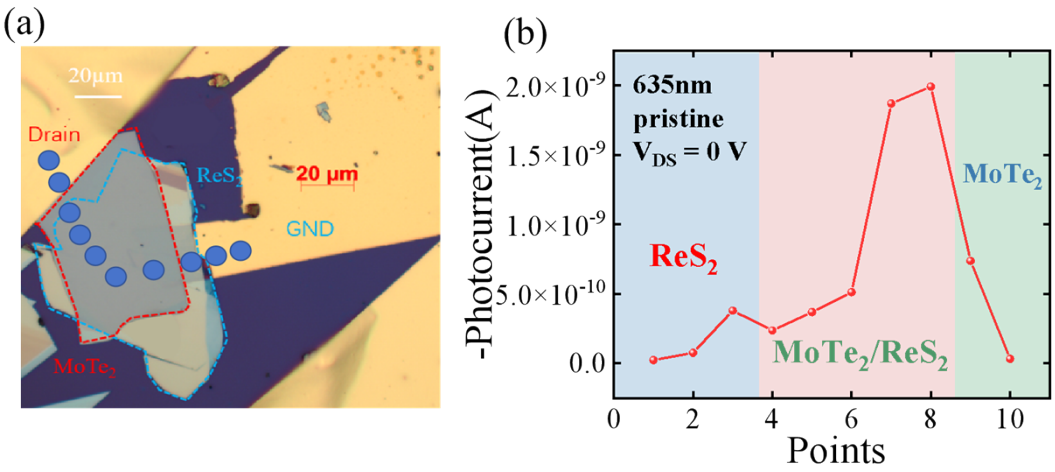

Figure S6 *(a,b) Spatial photocurrent line scans of the undoped heterojunction at V_{DS} = 0 V under 635 nm laser illumination. The blue-marked point indicates the laser focus position, with the scan direction denoted by the black arrow in the inset of (a).*

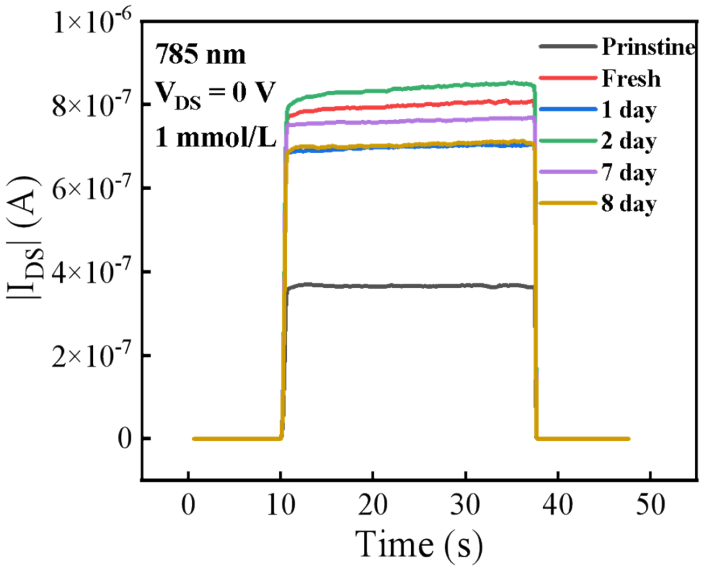

Figure S7 *The temporal photovoltaic response of the MoTe2/ReS2 photodetector after different days.*

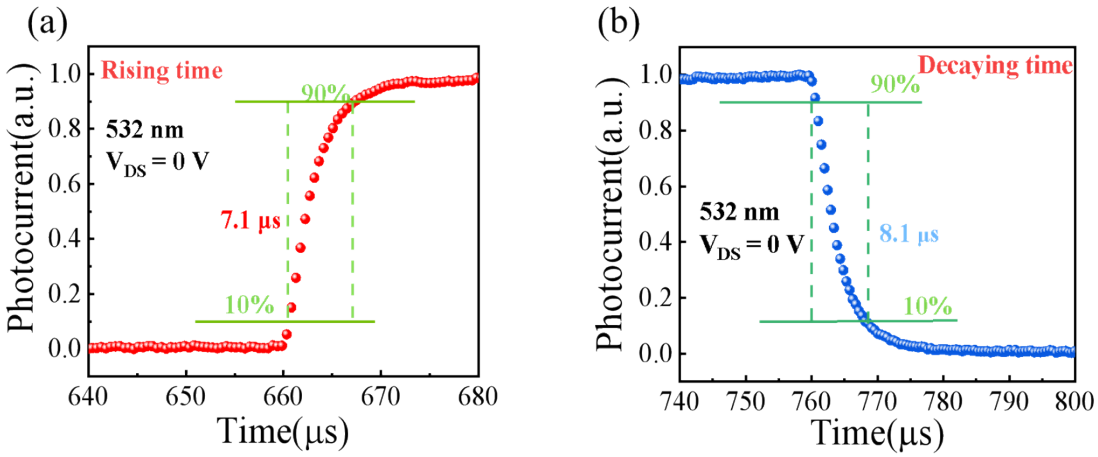

Figure S8 *(a,b) Rise and fall times of the undoped photodetectors under laser irradiation at 532 nm wavelengths.*